Open Framework and Microporous Transition Metal Silicates

Allan J. Jacobson, Xiqu Wang, Lumei Liu, and Jin Huang
Department of Chemistry, University of Houston
Houston, TX 77204, U.S.A.

ABSTRACT

A family of microporous and open-framework microporous transition metal silicates have been prepared by hydrothermal synthesis at $T \leq 240$ ºC. The structures of the compound are based on a common principle in which anionic silicate components (layers, chains, or cluster anions) are connected by isolated transition metal polyhedra by sharing four corners in a square arrangement. Known examples of this class of compounds are reviewed and some recent progress on extending the syntheses to include organic templates are discussed.

INTRODUCTION

Porous crystalline materials that contain cavities and channels with dimensions on the nanometer scale have a wide range of important applications in molecular separations, as ion-exchangers, and in heterogeneous catalysis. The aluminosilicates or zeolites that have structures based on frameworks of connected tetrahedral SiO_4 and AlO_4 building units are the most important class of porous crystals that have commercial applications. The aluminophosphates, substituted aluminophosphates, gallophosphates, and zinc and cobalt phosphates are other examples of 'zeotypes' based on tetrahedral building units that have been discovered in the last two decades in the search for new selective catalysts [1].

A second, though less explored, class of open-framework solids contains compounds with structures formed by linking tetrahedra with other types of metal ion centered polyhedra such as octahedra or square pyramids. A large number of mixed polyhedral frameworks containing phosphate groups have been synthesized but in contrast, relatively few silicates and germanates have been reported. though these are expected to have better stability over a wider range of catalytic conditions [2]. Several phases, for example the titanosilicate $Na_2TiSi_5O_{13}\cdot H_2O$ (ETS-10), have wide channel systems and substantial micropore volume.

We have recently focused on the synthesis of vanadium and other transition metal silicates because they are expected to show better thermal and hydrothermal stability than the corresponding phosphates. In contrast to the large family of vanadophosphates, only one synthetic large pore vanadosilicate (AM-6, isostructural with ETS-10) is known that contains silicate tetrahedra in combination with oxovanadium (IV) species that are an essential part of the framework [3]. We have obtained using mild hydrothermal synthesis conditions, a large family of open-framework and, in some cases microporous, transition metal silicates [4-9]. A new class of compounds (designated *MSH-nA* for *M*etal *S*ilicate *H*ouston-*nA*, where M is the specific transition metal, n is the framework type and A represents the non-framework cations) comparable to the zeolite family can be predicted based on the building units found in this series.

EXPERIMENTAL

The *MSH-n* compounds were synthesized by hydrothermal methods similar to those used in the synthesis of zeolites. Typically, a silica gel was mixed with solutions of the appropriate metal

salt ($VOSO_4 \cdot nH_2O$, $UO_2(NO_3)_2 \cdot 6H_2O$) and AOH (A = Na, K, Rb, Cs) and subsequently heated at 180-240 °C for 2-14 days under autogenous pressure in a 23 mL Parr hydrothermal reactor. After reactions, the pH values of the supernatant solutions were measured and the solid products were recovered by vacuum filtration and washed with water and methanol. A systematic approach using reaction mixture diagrams was used to determine the existence of new phases. Thereafter, the reactant ratios and temperature were adjusted to optimize the yield. In most cases, single phases were obtained in high yield. For some products, additional purification was necessary to remove unreacted silica gel. Crystals or microcrystalline powders of the different *MSH-nA* compounds were recovered depending on the specific alkali cation. Water contents of the products were determined by thermogravimetric analysis and the metal : Si ratios by electron probe microanalysis. Samples were further characterized by infrared, UV-vis absorption spectroscopy and by magnetic measurements.

X-ray single crystal analysis was performed on a Siemens SMART platform diffractometer (SAINT version 4.05) outfitted with a 1K CCD area detector and monochromatized graphite Mo-Kα radiation (Siemens Analytical X-ray Instruments, Madison, WI). Structures were determined by direct methods and refined using SHELXTL.

RESULTS

The crystal structures of the *MSH-n* series of compounds share a common building principle. They can be described as a combination of silicate anionic building units and isolated transition metal square cross-linking units. The silicate building units can be simple layers of composition $[SiO_{3/2}O_{1/1}]^-$, $[SiO_{2/2}O_{2/2}]^{2-}$ chains or cluster anions, or more complex units such as double layers and double chains. The silicate units are connected into a three dimensional framework by isolated transition metal polyhedra that share four oxygen atoms with the silicate component and have one or more unshared ligands, $MO_{4/2}X_n^{2+}$, n=1,2. Examples are known for the following linking transition metal units $ZrO_{4/2}F_2^{2+}$, $VO_{4/2}O_{1/1}^{2+}$, $NbO_{4/2}F_{1/1}O_{1/1}^{2+}$, $UO_{4/2}O_{2/1}^{2+}$, $CuO_{4/2}(H_2O)_{2/1}^{2+}$ and the dimer $[VO_{2/2}O_{2/3}O_{1/1}]_2^{4+}$. The transition metal cationic units connect to the silicate units by forming three-rings in the *VSH-n* series and three, four and five rings in the *USH-n* family. The combined transition metal silicate frameworks have net negative charges and, analogous to zeolite structures, contain alkali metal charge balancing cations that are usually solvated. Examples of the bridging units found in *VSH-9* and *USH-5* are shown in Figure 1. Examples of the *MSH-n* series are given in Table I

The *VSH-nA* structures are all based on silicate layers bridged by VO^{2+} ions to form frameworks; water molecules and non-framework A^+ cations fill the intracrystalline pore space. Except for *VSH-2Cs*, the *VSH-nA* structures contain single silicate layers with the composition $Si_2O_5^{2-}$ ($SiO_{3/2}O_{1/1}^-$) that can be represented by three-connected plane nets to describe the possible arrangements of the tetrahedra within each single silicate layer (see Table I). Specific examples are shown in Figures 2 and 3 to illustrate the general principle.

Silicate layers with different orientations of the SiO_4 tetrahedra (either up or down) can correspond to the same 3-connected plane net. Thus the layers of *VSH-1*, *VSH-3*, *VSH-14* and pentagonite differ from each other in the orientation of the terminal oxygen atoms, but all correspond to the plane net 6^3. A single type of silicate layer is found in all structures except in the structure of *VSH-11* which has two different silicate layers (designated L4a and L4b) both corresponding to the plane net (4.6.8)(4.8.12).

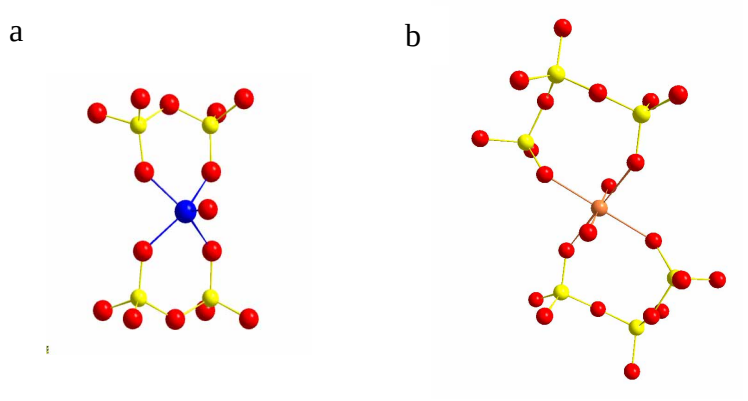

Figure 1. Examples of transition metal cation linking groups a) $VO_{4/2}O_{1/1}^{2+}$ forming three-rings and b) $UO_{4/2}O_{2/2}^{2+}$ forming four-rings

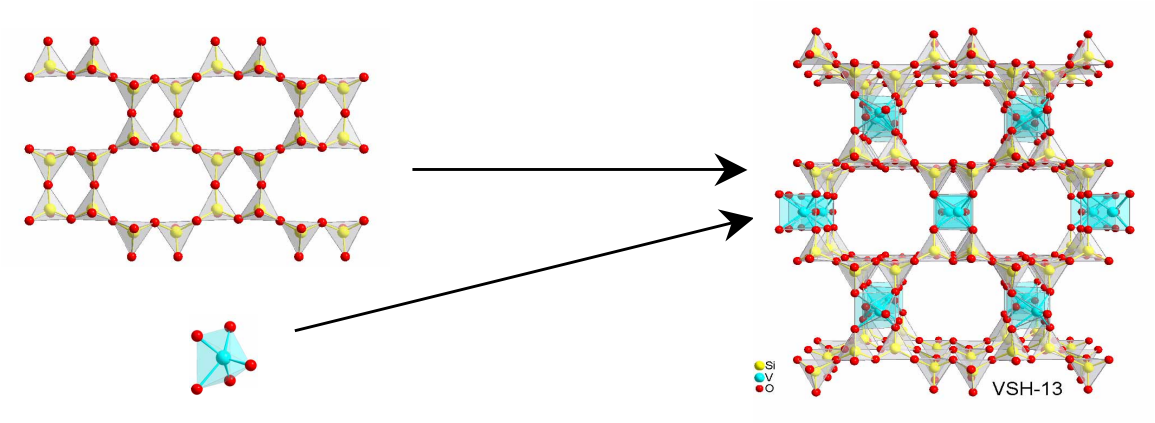

Figure 2. A schematic illustration of the formation of $Na_2(VO)Si_4O_{10}\cdot 3H_2O$, *VSH-13Na* from a silicate layer L2b [4.8^2] and a $VO_{4/2}O_{1/1}^{2+}$ connecting unit

VSH-n phases can also be described in terms of stacking of layers, an approach that is particularly useful for understanding relationships between different structures and disorder and is illustrated for the case of the 6_3 L3 layer in *VSH-4*, *6*, and *9*. In *VSH-4*, each layer is shifted by (*a*-*b*)/3 relative to its neighbors, therefore the stacking sequence is *ABC*. *AB* stacking of the L3 layer requires a non-equivalent arrangement of the interlayer pyramids on the two sides of the layer and has not been observed. The non-equivalency of the pyramid arrangement can be avoided, however, in $\overline{AB}$ stacking, where the neighboring layers are related by a glide plane with a translation (*a*-*b*)/3. The structure of *VSH-6* was refined with an ordered $\overline{AB}$ stacking model, although the crystal showed strong diffuse reflections indicating some stacking disorder. An ordered *ACB* stacking of the L3 layer is observed in *VSH- 9*. The stacking sequences *ABC* and *ACB* are not equivalent because the layers are non-planar. Different interlayer arrangements of the bridging VO^{2+} and different channels in the structure are a consequence. In principle, the layers L3 can also be stacked in *AA* or $\overline{AA}$ sequences lead to framework structures with one-dimensional 12-ring channel systems along the stacking direction and 8-ring or 10-ring channels parallel to the layers, respectively. We have not yet observed these stacking sequences.

Table I A survey of open framework and microporous transition metal silicates: MSH-n

Name	Formula	Space group	silicate layer, net	Ref.
VSH-n				
VSH-1K	$K_2(VO)(Si_4O_{10})\cdot H_2O$	Pbca	L1a, 6^3	4
VSH-2Cs	$Cs_2(VO)(Si_6O_{13})\cdot 3H_2O$	Cmca	L5, $4^2.6+4.6^2$	4
VSH-3Rb	$Rb_2(VO)_2(Si_6O_{15})\cdot 1.6H_2O$	$Cmc2_1$	L1b, 6^3	5
VSH-3K	$K_2(VO)_2(Si_6O_{15})\cdot 1.6H_2O$	$Pbc2_1$	L1b, 6^3	5
VSH-4Cs	$Cs_2(VO)(Si_4O_{10})\cdot 2.7H_2O$	R-3m	L3, 6^3	5
VSH-4Rb	$Rb_2(VO)(Si_4O_{10})\cdot 3H_2O$	R-3m	L3, 6^3	5
VSH-6CsK	$(Cs,K)_2(VO)(Si_4O_{10})\cdot 3H_2O$	P31c	L3, 6^3	5
VSH-6Rb	$Rb_2(VO)(Si_4O_{10})\cdot 3H_2O$	$P6_3/mmc$	L3, 6^3	5
VSH-9CsNa	$CsNa(VO)(Si_4O_{10})\cdot 4H_2O$	R3m	L3, 6^3	5
VSH-11RbNa	$(Rb,Na)_2(VO)(Si_4O_{10})\cdot xH_2O$	R-3m	L4a, L4b, 4.6.8+4.8.12	5
VSH-12Cs	$Cs_2(VO)(Si_4O_{10})\cdot xH_2O$	Pbam	L2a, 4.8^2	5
VSH-12LiX	$Li_2(VO)(Si_4O_{10})\cdot xH_2O$	Pbam	L2a, 4.8^2	5
VSH-13Na	$Na_2(VO)(Si_4O_{10})\cdot 3H_2O$	Imma	L2b, 4.8^2	5
VSH-14Na	$Na_2(VO)(Si_4O_{10})\cdot 1.4H_2O$	C2/c	L1a, 6^3	5
USH-n				
USH-1Na	$Na_2(UO_2)(Si_2O_6)\cdot 2.1H_2O$	C2/m	L5, $4^2.6+4.6^2$	7
USH2-Rb	$Rb_4(UO_2)_2(Si_8O_{20})$	P-1	double chains	8
USH3-RbNa	$RbNa(UO_2)(Si_2O_6)\cdot H_2O$	P-1	tetramer	7
USH4-Rb	$Rb_2(UO_2)(Si_2O_6)\cdot H_2O$	P21/n	teramer	8
USH5-Rb	$Rb_2(UO_2)(Si_2O_6)\cdot 0.5H_2O$	Pbca	single chains	8
USH5-Cs	$Cs_2(UO_2)(Si_2O_6)\cdot 0.5H_2O$	Pbca	single chains	8
USH-7K	$K_6(UO_2)_3(Si_8O_{22})$	C2/m	tetramer	9
CSH-n				
CSH-1Na	$Na_4[Cu_2Si_{12}O_{27}(OH)_2]\cdot 6H_2O$	Cmcm	double layers	9
CSH-2Na	$Na_2[Cu_2Si_4O_{11}]\cdot 2H_2O$	P-1	double chains	9

We designate the metal silicate family *M*etal *S*ilicate *H*ouston-*nA* (*MSH-nA*), where M is the specific transition metal, n is the framework type and A represents the non-framework cations.

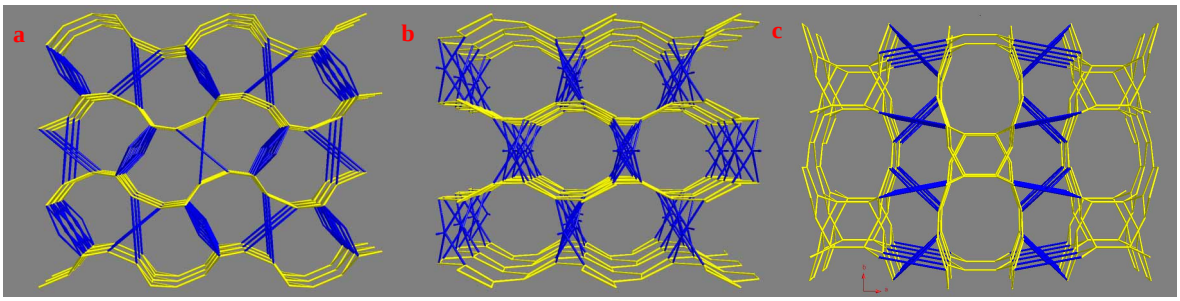

Figure 3 Channel systems in representative *MSH–n* compounds a) 9-ring channels in *VSH-12*, b) 10-ring channels in *VSH-13*, and c) 12-ring channels in *CSH-1*. Si and M atoms are at the vertices of the nets and oxygen atoms are omitted.

The *USH-n* series have new open-framework structures without mineral analogs that contain a greater diversity of condensed silicate units (Table I). Examples have been found where UO_6 tetragonal bipyramidal units connect the L5 layer, double chains, 4-membered rings, and single chains of SiO_4 tetrahedra. Unlike the *VSH-n* compounds which contain only VSi_2 three rings, in the *USH-n* series 3, 4, and 5 member rings are observed (see Figure 1). Most likely, the difference arises from the larger size of the uranium cation that permits a greater range of O-O distances in the basal plane the $UO_{4/2}O_{2/1}^{2+}$ tetragonal bipyramidal units. Tetragonal bipyramidal coordination is the only geometry observed for U atoms in the *USH-n* compounds. In contrast the normal environment typically found in mineral structures is seven-coordination. For example, chains of edge shared UO_7 pentagonal bipyramids are linked by SiO_4 tetrahedra to form layers in the structures of uranophane, $Ca[UO_2]_2[SiO_3(OH)]_2{\cdot}5H_2O$, sklodowskite, $Mg[UO_2]_2[SiO_4]_2{\cdot}7H_2O$, boltwoodite, $K[H_3O][UO_2][SiO_4]$, and kasolite, $PbUO_2SiO_4{\cdot}H_2O$.

The *CSH-n* series of compounds is less well developed at this time and only *CSH-1* will be briefly discussed. The porous framework of the structure *CSH-1*, $Na_4[Cu_2Si_{12}O_{27}(OH)_2]{\cdot}6H_2O$ is built from silicate double layers cross-linked by $[CuO_4(H_2O)_2]$ octahedra (Figure 3b). The silicate double layer contains wide channels defined by 12-rings of tetrahedra with an aperture 7.3 x 4.4 Å, and perpendicular 8-ring channels with an aperture 3.8 x 2.5 Å. The channels are filled by disordered water molecules. The sodium ions are located between the double layers.

Preliminary studies show that the *VSH-n* frameworks have 'zeolitic' properties that are consistent with their structures. As examples, *VSH-4* and *VSH-9* show excellent thermal stabilities (to 500 ºC) and reversible dehydration-rehydration properties as confirmed by X-ray powder diffraction and thermogravimetric analysis. In Figure 4, data on the thermal stability of *VSH-9* are shown as an example. A sample was heated for 1 h in either flowing nitrogen gas or in nitrogen containing 3% oxygen. After heating, the sample was cooled to room temperature and characterized by powder X-ray diffraction. The process was then repeated with the same sample at increments in temperature of 100 ºC. The results show that in nitrogen the sample does not lose significant

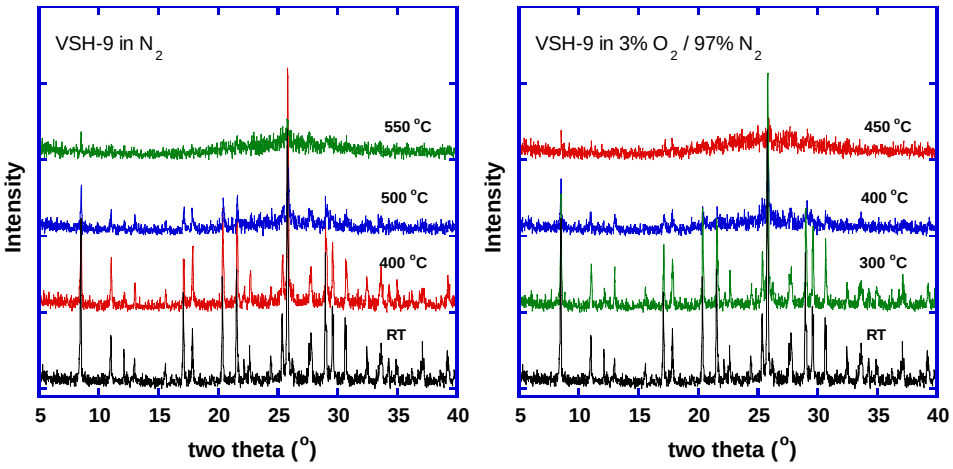

Figure 4 Effects of heat treatment on the crystallinity of *VSH-9* in N_2 and in N_2 / 3% O_2

crystallinity until above 500 ºC. Loss of crystallinity occurs at lower temperature 400 ºC in the presence of O_2 presumably due to oxidation of the bridging VO^{2+} with an accompanying change in coordination. Enhanced water absorption capabilities were observed after exchange of Li^+ for the larger alkali cations. The nitrogen absorption isotherms for *VSH-9CsNa* and *VSH-9LiX* show

type 1 absorption indicative of true microporosity. The partial removal of Cs by ion exchange results in a significant increase in the volume of nitrogen absorbed from 25 mL^3g^{-1} to 125 mL^3g^{-1}.

CONCLUSION

The *MSH-n* compounds were synthesized by using alkali metal cations as templating agents. In the development of zeolite synthesis, however, introduction of organic templates greatly increased the topology and composition spectrum of zeolite structure. Consequently, we are currently investigating a similar approach to metal silicates but with the addition of fluoride ions in order to enhance the solubility of silicate species in the presence of only organic bases. The first reported example that falls into the general family of compounds is the fluorogermanate $Ge_2ZrO_6F_2{\cdot}(H_2DAB){\cdot}H_2O$ ASU-15 in which single germanate chains are connected by $ZrO_{4/2}F_2^{2+}$ cations [10]. Subsequently, we prepared by using the similar sized template, diaminocyclohexane, *NGH-5*, in which the same chains are bridged by $NbO_{4/2}F_{1/1}O_{1/1}^{2+}$cations [11]. Both structures are closely related to that of *USH-5A* that contains only inorganic cations. Most recently, we have successfully synthesized the firs silicate example $[(CH_3)_4N][(C_5H_5NH)_{0.8}((CH_3)_3NH)_{0.2}]U_2Si_9O_{23}F_4$ *USH-8* [12]. In the structure of *USH-8*, double silicate layers of the type found in ferrierite are linked by infinite chains of composition $UO_{2/2}O_{1/2}F_{4/2}$. Tetramethyl ammonium, dimethylammonium and pyridinium cations occupy the asymmetric pore space. The successful use of organic templates in this synthesis suggests further opportunities for synthesizing microporous metal silicates in a systematic way.

ACKNOWLEDGEMENTS

This work was supported by the National Science Foundation under Grant DMR-0120463 and by the Robert A. Welch Foundation. This research was also supported through the use of the Center for Materials Chemistry Shared Experimental Facilities.

REFERENCES

1. For a recent review see A. K. Cheetham, G. Férey, T. Loiseau, *Angew. Chem. Int. Ed., Engl*. 38, 3268, (1999).
2. J. Rocha, M. W. Anderson, *Eur. J. Inorg. Chem.*, 801, (2000).
3. J. Rocha, P. Brandão, Z. Lin, M. W. Anderson, V. Alfredsson, O. Terasaki, *Angew. Chem. Int. Engl.*, 36, 100, (1997).
4. X. Wang, L. Liu, A. J. Jacobson, *Angew. Chem. Int. Ed.*, 40, 2174, (2001).
5. X. Wang, L. Liu, A. J. Jacobson, *J. Amer. Chem. Soc.*, 124, 7812, (2002).
6. J. Huang, X. Wang, L. Liu, A. J. Jacobson, *Solid State Sciences*, 4, 1193, (2002).
7. X. Wang, J. Huang, L. Liu, A. J. Jacobson, *J. Mater. Chem.*, 12, 406, (2002).
8. J. Huang, X. Wang, A. J. Jacobson, *J. Mater. Chem.*, (2002) in press.
9. X. Wang, J. Huang, L. Liu, A. J. Jacobson, unpublished results.
10. H. Li, M. Eddaoudi, J. Plevert, M. O'Keefe, O. M. Yaghi, *J. Am. Chem. Soc.*, 122, 12409 (2000).
11. R. J. Francis, A. J. Jacobson, *Chem. Mater.* 13, 4676, (2001)
12. X. Wang, J. Huang, and Allan J. Jacobson, *J. Amer. Chem. Soc.* (2002) in press.